Materials Advances

PAPER

View Article Online
View Journal | View Issue

Check for updates

Cite this: *Mater. Adv.*, 2022, 3, 4608

Preparation and characterisation of zwitterionic sulfobetaine containing siloxane-based biostable polyurethanes†

Zhi-hua Liu,[a] Yong-hao Xiao,[a] Xiao-yu Ma,[a] Xue Geng,[ab] Lin Ye,[ab] Ai-ying Zhang[ab] and Zeng-guo Feng *[ab]

Received 18th January 2022,
Accepted 14th April 2022

DOI: 10.1039/d2ma00049k

rsc.li/materials-advances

Siloxane-based biostable polycarbonateurethanes (PCUs) with varying [PDMS]/([PDMS] + [PCDL]) were synthesized by a two-step solution polymerisation method. As potential blood-contact biomaterials, their biocompatibility was further improved by inserting sulfobetaine *via* three synthetic protocols. It was found that Mn was progressively decreased from 4.50×10^4 to 3.23×10^4 with increasing PDMS content and the PDI was kept below 2.0 after the zwitterionic modification. At the same time, the Mn was reduced from 3.78×10^4 for a 20 mol% PDMS containing PU to around 2.38×10^4 for these zwitterion modified PUs while the PDI was dropped below 1.61. Accordingly, the tensile stress was dropped from 43.1 MPa to about 25.3 MPa and the fracture energy was decreased from 146.4 MN m^{-1} to about 69.8 MN m^{-1}. Thanks to the enrichment of PDMS on the surface as evidenced by XPS analysis, the water contact angle (WCA) was increased from 106.2° to 116.8°, whereas this value was again decreased to about 94.6° after inserting sulfobetaine. Compared to siloxane-based PCUs, the fibrinogen absorption on and platelet adhesion to the surface of these zwitterionic modified ones were markedly retarded. This suggested that there is a trade-off between the mechanical properties and biocompatibility for the zwitterion containing siloxane-based biostable PCUs applied as blood-contacting biomaterials.

Introduction

Polyurethane (PU) is a general term for a class of urethane-containing polymer materials.[1] It is mainly composed of soft segments and hard segments. This unique structure endows it with not only good mechanical properties, but also the structure which can be flexibly adjusted according to specific requirements.[2] For instance, its robust ability to formulate biomaterials with a broad range of mechanical properties and favourable biocompatibility has attracted tremendous interest for newly emerging biomedical applications.[3] However, there is still an unavoidable issue that its partial degradation always occurs under the action of enzymes and active oxygen species in the human body when it is employed as a long-term implantable material[4]. Extensive fundamental and experimental studies have elucidated that the *in vivo* degradation of PUs is mostly hydrolysis and oxidative degradation.[5–7] For example, polyester-based PUs are prone to hydrolytic degradation, while polyether-based ones are prone to oxidative degradation, highly limiting their long-term implantation applications.[8] After more than 60 years of research and development, there emerges one way capable of boosting the biostability of either polyester-based or polyether-based PUs, *i.e.* polycarbonate (PC) completely replacing polyester or polyether to give biostable PC-based polyurethanes (PCUs).[4,9–11] Even so, their *in vitro* and *in vivo* degradations still remain a concern due to a possible slow hydrolysis of carbonate linkages under the physiological conditions.[4,12,13]

As the method of choice to combine the merits of good long-term biostability and biocompatibility and observed mechanical properties, polydimethylsiloxane (PDMS) can be incorporated, but it generally needs PC as a co-soft segment for improving the compatibility between PDMS soft and hard segments of the siloxane-based PCUs.[14–17] PDMS is well known for its non-reactivity, stability and resistance to extreme environments, retaining useful properties for applications in a broad temperature range from −55 °C to 300 °C, low moisture permeability, and good oxidative and hydrolytic stability. It was shown that the incorporation of PDMS as a co-soft segment has endowed

[a] School of Materials Science and Engineering, Beijing Institute of Technology, Beijing 100081, China
[b] Beijing Key Laboratory of Construction Tailorable Advanced Functional Materials and Green Applications, Beijing 100081, China

† Electronic supplementary information (ESI) available. See DOI: https://doi.org/10.1039/d2ma00049k

the PCUs with attractive properties such as low glass transition temperature, excellent hydrolytic and oxidative stability, good blood compatibility, low toxicity and anti-fouling characteristics due to their low surface energy. As a result, the attainment of both long-term biostability and observed mechanical properties is never unavailable for PCUs as long-term implantable biomaterials by mixing PDMS as one of the co-soft segments.[10,18]

Although the siloxane-based biostable PCUs possess good long-term biostability and biocompatibility, their anticoagulant and antithrombotic characters are far from perfect when they are used as blood-contacting biomaterials. Up to now many attempts have been made to reduce coagulation and thrombosis of medical PUs, for example, hyperhydrophobicity,[19,20] hydrophilicity,[21] heparinisation,[22–24] zwitterionic modification[25,26] and biomimetic design strategies.[27–29] It should be noted that most of these anticoagulant and antithrombotic strategies improve the biocompatibility of medical PUs as blood-contacting biomaterials through surface modification. There are a few studies on the bulk modification of PUs from the very beginning of step-growth polymerisation. Sulfobetaine is a typical betaine zwitterionic monomer whose positive and negative charge groups are held on the same molecule.[30] Betaines usually include phosphate betaine, sulfonate betaine and carboxylate betaine. Among them, the sulfobetaine amphoteric monomer has received increasingly growing attention because of its good chemical and thermal stability and strong hydration ability.[25,26,31–33] Nowadays various zwitterionic polymers are broadly used in the fabrication or coating of long-term blood-contacting medical devices, such as small diameter vascular grafts, arteriovenous access, artificial lungs, and microfluidic devices for their good hydration properties and strong anti-fouling ability.[26,34,35] Meanwhile, the mechanism of zwitterionic polymers, how to reduce and impede protein adsorption and platelet deposition, has also been illuminated recently.[25,33,36] Herein in order to booster the biocompatibility and biostability of PCUs as potential blood-contacting biomaterials, a varying amount of PDMS was first allowed to mix with PC to synthesize siloxane-based PCUs through a two-step solution polymerisation method and subsequently sulfo-betaine was incorporated into their backbones ***via*** three synthetic protocols. In addition to the effects of introduction of siloxane and zwitterionic sulfobetaine on the molecular weight and mechanical properties, their biocompatibility was also evaluated in this study.

Materials and methods

Materials

Poly(1,6-hexyl carbonate) diol (PCDL) (M_n = 2000) purchased from Ube Industries Co., Ltd (Japan) and α,ω-bis(hydroxylethoxy-propyl) polydimethylsiloxane (PDMS) (M_n = 2000) provided by Merida (Beijing, China) were dried in vacuum at 120 °C for 2 h before use; 4,4′-dicyclohexylmethane (HMDI) was purchased from Innochem (Beijing, China) and 1,4-butanediol (BDO) from Macklin Inc. (Shanghai, China), respectively; Ultra-dry dichloroethane (DCE), *N*,*N*-dimethylacetamide (DMAc) and dimethyl sulfoxide (DMSO) all with $H_2O \leq 50$ ppm were bought from Energy Chemical (Shanghai, China); dibutyltin dilaurate was provided by Aladdin (Shanghai, China); 1,3-propanesultone (PS) was obtained from Innochem (Beijing, China); *N*-methyldiethanolamine (MDEA) was purchased from Energy Chemical (Shanghai, China); hexafluoroisopropanol (HFIP) was purchased from Sigma-Aldrich (USA); tetrahydrofuran (THF) and hydrogen peroxide (30%) were purchased from Innochem (Beijing, China). All the other chemical reagents and solvents were of analytical grade unless otherwise specified.

Synthesis of siloxane-based PC PUs

For convenience, all the siloxane-based PCUs using PDMS and PCDL as co-soft segments were expressed as PD*x*, where *x* is the molar fraction of PDMS to PDMS and PCDL. As a typical sample, the synthesis of 20 mol% PDMS containing PCU is as follows. 1.6 g (0.8 mmol) PCDL and 0.4 g (0.2 mmol) PDMS were added to the reaction vessel to dehydrate with mechanical stirring under reduced pressure in an oil bath at 120 °C for 1 h. Nitrogen protection was used throughout the reaction process. Thereafter, the temperature was reduced to 75 °C, an appropriate amount of DMAc was added keeping the solution concentration at 15 wt%, and 1.32 g (5 mmol) HMDI was introduced into the reaction vessel. After 6 h of prepolymerisation, 0.27 g (3 mmol) BDO and 0.5 wt% dibutyltin dilaurate were added, and the temperature was adjusted to 85 °C for 12 h. The obtained polymer solution was placed for 12 h and then poured into a water/methanol (1 : 1) solution for precipitation, and rinsed several times with a water/methanol (1 : 1) solution to remove low molecular weight substances such as solvents and impurities. Finally, the obtained PD20 was dried in a vacuum drying oven at 60 °C for three days and kept for later use.

Synthesis of zwitterionic sulfobetaine inserted PUs

The resulting PD20 was selected for further zwitterionic modification *via* the following three protocols.

Protocol one. 1.6 g (0.8 mmol) PCDL and 0.4 g (0.2 mmol) PDMS were added to the reaction vessel, and then dehydrated with mechanical stirring under reduced pressure in an oil bath at 120 °C for 1 h. Nitrogen protection was used throughout the reaction process. Thereafter the temperature was reduced to 75 °C, an appropriate amount of DMAc was added keeping the solution concentration at 15 wt%, and 1.32 g (5 mmol) HMDI was introduced into the reaction vessel. After 6 h of prepolymerisation, 0.135 g (1.5 mmol) BDO, 0.179 g (1.5 mmol) MDEA and 0.5 wt% dibutyltin dilaurate were added, and the temperature was increased to 85 °C for 12 h. The obtained polymer solution was placed for 12 h and then poured into a water/methanol (1 : 1) solution for precipitation, and rinsed several times with a water/methanol (1 : 1) solution to remove solvents, impurities and other low molecular weight substances. The obtained MDEA containing MDEA-PD20 was dried in a vacuum drying oven at 60 °C for three days. The dried 2 g MDEA-PD20 was dissolved in the DCE/THF mixed solution and placed in an oil bath at 50 °C. Then 0.3 g (2.5 mmol) PS was added to the solution and reacted overnight. The solution was precipitated with excess methanol. The resulting zwitterion modified siloxane-based PCU was designated as S1PD20. It was dried in a vacuum drying oven at 60 °C and kept for later use.

Protocol two. Sultaine diol (SB-MDEA) was synthesized and characterised according to the literature[36] and the analytical results are shown in Fig. S1–S3 (ESI†).

1.6 g (0.8 mmol) PCDL, 0.4 g (0.2 mmol) PDMS and 0.36 g (1.5 mmol) SB-MDEA were added to the reaction vessel and then dehydrated with mechanical stirring under reduced pressure in an oil bath at 120 °C for 1 h. Nitrogen protection was used throughout the reaction process. Thereafter the temperature was reduced to 75 °C, an appropriate amount of DMSO was added keeping the solution concentration at 15 wt%, and 1.32 g (5 mmol) HMDI was introduced into the reaction vessel. After 6 h of prepolymerisation, 0.135 g (1.5 mmol) BDO and 0.5 wt% dibutyltin dilaurate were added, and the temperature was again increased to 85 °C for 12 h. The obtained polymer solution was placed for 12 h and then poured into a water/methanol (1 : 1) solution for precipitation, and rinsed several times with a water/methanol (1 : 1) solution to remove low molecular weight substances such as solvents and impurities. The resulting zwitterion modified PU was designated as S2PD20 and further dried in a vacuum drying oven at 60 °C for later use.

Protocol three. 1.6 g (0.8 mmol) PCDL and 0.4 g (0.2 mmol) PDMS were added to the reaction vessel and then dehydrated with mechanical stirring under reduced pressure in an oil bath at 120 °C for 1 h. Nitrogen protection was used throughout the reaction process. Thereafter the temperature was reduced to 75 °C, an appropriate amount of DMSO was added keeping the solution concentration at 15 wt%, and 1.32 g (5 mmol) HMDI was introduced into the reaction vessel. After 6 h of prepolymerisation, 0.135 g (1.5 mmol) BDO, 0.36 g (1.5 mmol) SB-MDEA and 0.5 wt% dibutyltin dilaurate were concomitantly added, and the temperature was then adjusted to 85 °C for 12 h. The obtained polymer solution was placed for 12 h and then poured into a water/methanol (1 : 1) solution for precipitation, and rinsed several times with a water/methanol (1 : 1) solution to remove low molecular weight substances such as solvents and impurities. The resulting zwitterion modified PU was designated as S3PD20, and then dried in a vacuum drying oven at 60 °C for later use.

Preparation of PU films

0.3 mm thick films were made of siloxane-based PCUs cast in a 10% (w/v) solution in HFIP. The completely dissolved PU solution was poured into a glass mould and placed in a ventilated place at room temperature for 24 h. Then the cast films were further dried under vacuum at 60 °C for 3 days, and finally dried in a forced air oven at 60 °C for 3 days. These PCU samples were stored in a desiccator at room temperature for two weeks before characterisation.

Fourier transform infrared (FTIR) spectroscopy

The FTIR measurements were carried out using a Shimadzu IRTrace-100 FTIR infrared spectrometer in a transmission mode. The background used was KBr, the testing temperature was set at 25 °C, the resolution was 4 cm^{-1}, and the number of scans was 30 times.

^{1}H NMR spectroscopy

The chemical structure of the zwitterionic siloxane-based PCUs was confirmed by ^{1}H NMR analysis on a Bruker ARX 400 spectrometer using DMSO-d_6 and D_2O as solvents.

Molecular weight determination

The molecular weights and molecular weight distributions of the samples were determined by gel permeation chromatography (GPC) analysis on a HLC-8320GPC (TOSOH, Japan) chromatograph using DMF as the eluent. The molecular weight was relative to the polystyrene standard. The sample concentration was set at 10 mg mL^{-1}, the flow rate was kept at 0.3 mL min^{-1}, and the testing temperature was 40 °C.

Mechanical performance tests

The tests on the mechanical properties of all the resulting PUs were carried out using a DXLL-5000 electronic universal testing machine (Shanghai, China) at 25 °C, and the tensile rate was 20 mm min^{-1}. Each sample was cut into a dumbbell with a length of 5 cm and a width of 1 cm; the effective part was stretched: the length was 20 mm, the width 4 mm, and the thickness about 0.3 mm. The testing result was the average of five repetitions.

Dynamic thermomechanical analysis (DMA)

The glass transition temperature (T_g) and storage modulus (E') of the selected PU samples were analysed by dynamic thermomechanical analysis. The instrument used was DMA-Q800 (TA Instruments, USA), and the test conditions were test temperature −140 °C to 140 °C, shaking and stretching mode, frequency 10 Hz, heating rate 5 °C min^{-1}, and atmospheric air.

Static water contact angle (WCA) test

The static water contact angle (WCA) was tested by the sessile drop method using a JC2000C1 static drop contact angle/interfacial tension tester (Shanghai, China) at room temperature. Each sample was tested three times.

Scanning electron microscopy (SEM) analysis

The morphology of the PU surface was characterized by SEM. The instrument used in the test was a Hitachi S-4800 scanning electron microscope (Japan). All the samples were sprayed with gold to improve conductivity before testing.

X-ray photoelectron spectroscopy (XPS) analysis

XPS was used for the surface elemental composition of the selected PUs to characterize their surface properties. The instrument used was Phi Quantera-II SXM (UlvacPhi, Japan), and the X-ray source was AlKa (Al target, 1486.6 eV, line width 0.68 eV). The 10 nm depth of the PU surface was analysed by setting the take-off angle at 90°, and different take-off angles were used to achieve the purpose of measuring the depths of 4 nm and 7 nm.

Determination of the water absorption ratio

The water absorption of the PU samples was characterized by immersing the film in phosphate buffered saline (PBS) at room temperature and absorbing water for 48 h at 37 °C. After 48 h, the sample was taken out of the buffer, and at the same time the water attached to the surface was sucked away with filter paper. The water absorption is calculated as the average of the three measured values. The water absorption ratio (%) is calculated using formula (1).

$$\mathrm{WA}\ (\%) = \frac{W_1 - W_0}{W_0} \times 100\% \tag{1}$$

where W_1 is the weight of the water-absorbing saturated polymer film, and W_0 is the weight of the dried polymer film.

Activated partial thromboplastin time (APTT) measurements

APTT is used to characterize the anticoagulant properties of the resulting PUs. The instrument used was a semi-automatic coagulometer (TEChrom IV plus, China). A PCU film was cut into a size of 4 × 6 mm, it was attached to the bottom of the quadruple lotus cup, 50 μL of plasma and 50 μL of kaolin were added, 50 μL of calcium chloride was added after 3 minutes, and the clotting time was recorded. Each sample was measured in four groups and the average value was taken. The corresponding reagents were purchased from Shanghai Long Island Biotec. Co., Ltd (Shanghai, China), and the anticlotting plasma came from the laboratory self-made.

Non-specific protein adsorption experiment (bovine fibrinogen as a model protein)

The surface protein adsorption on the PU film was evaluated by the Micro BCA protein assay. The material was cut into circular membrane samples with a diameter of 6 mm, and then the circular membrane samples were immersed in 5 mL of 0.03 g/100 mL fibrinogen solution, the test tubes were gently shaken for 3 h, the fibrinogen solution was drained, and then PBS was used to rinse the samples removing unadhered fibrinogen. After cleaning, round-bottomed test tubes were used to immerse the samples in 1 mL of 1 wt% sodium dodecyl sulfate (SDS) solution, and they were shaken at room temperature for 3 h to separate and dissolve the adsorbed protein in the aqueous SDS solution. From the above solution, 150 μL was taken and transferred to a 96-well plate. The diluted fibrinogen standard solution and Micro BCA work reagent were prepared according to the instructions of the Micro BCA protein determination kit and incubated at 37 ± 1 °C for 2 h. A microplate reader (ZS-2, Beijing Xinfeng Electrical Company, China) was used to read the absorbance at 562 nm to determine the amount of adsorption.

Platelet adhesion test (sheep blood as a model)

Whole sheep blood was collected by jugular vein puncture. *In vitro* thrombotic deposition on the PU samples was assessed by a simple rocking test using heparinised sheep blood. Each type of PU film was cut into 6 mm diameter discs, sterilised with ethanol, and then placed in a test tube. The test tube was filled with 4 mL of anti-coagulant sheep blood and gently shaken on the blood mixer at 37 °C for 3 h. After contact with sheep blood, the surface of the PU film was rinsed with PBS (10 times) to remove any unattached blood contents. The number of deposited platelets on the samples was quantified by LDH assay and further observed using a scanning electron microscope. For LDH activity assay, each washed sample was immersed in 1 mL of 2 wt% Triton-X 100 in PBS and then stirred for 20 min to lyse the deposited platelets on the sample. The lysis solution was centrifuged at 250 g for 10 min and then its supernatant was reacted with the LDH reagent. The absorbance of the reacted solution was recorded at 490 and 610 nm to quantify the amount of platelet deposited. To observe the morphology of the deposition of platelets on the surface of samples, after washing, the attached platelets were fixed by immersing in 2.5% glutaraldehyde solution for 2 h. The fixed platelets were dehydrated using 30, 50, 75, 95, and 100% EtOH. And SEM images were taken after sputter coating with gold/palladium.

Hemolysis test (rabbit blood as a model)

When the PU film was in direct contact with blood, the hemoglobin released by red blood cells was measured to determine its degree of hemolysis *in vitro*. 3.8 wt% sodium citrate was added to fresh rabbit blood to prepare anticoagulant rabbit blood, in which the mass ratio of the anticoagulant to rabbit blood is 1 : 9. The PU film was cut into a circular membrane sample with a diameter of 6 mm as the experimental group, and physiological saline and 1 wt% Triton-X100 were used as the negative and positive control groups, respectively. After incubating the experimental group and the control group with an equal mass of anticoagulant rabbit blood for 1 hour at 37 °C, they were centrifuged at 3000 rpm for 20 minutes. Then 100 μL of supernatant was added to the cuvette, and 700 μL of 2% sodium carbonate solution was also added. The absorbance was measured at a wavelength of 545 nm (UV-1800, Shimadzu, Japan). The calculation formula of the hemolysis ratio (HR%) is as follows:

$$\mathrm{HR}\ (\%) = \frac{A_1 - A_3}{A_2 - A_3} \times 100\% \tag{2}$$

where A_1, A_2, and A_3 are the absorption values of the experimental group, the positive control group and the negative control group, respectively.

Results and discussion

Synthesis and structural characterisation

Synthesis and characterization of SB-MDEA are described in the ESI† and Fig. S1–S3. As displayed in the schematic description in Scheme 1, siloxane-based PCUs using HMDI and BDO as the hard segments accounting for about 33% hard segment content and PDMS and PCDL as the co-soft segments with [PDMS]/([PDMS] + [PCDL]) in the range of 0–40 mol% were synthesized by a two-step solution polymerisation method. The molecular weight and polydispersity index (PDI) of the resulting PCUs

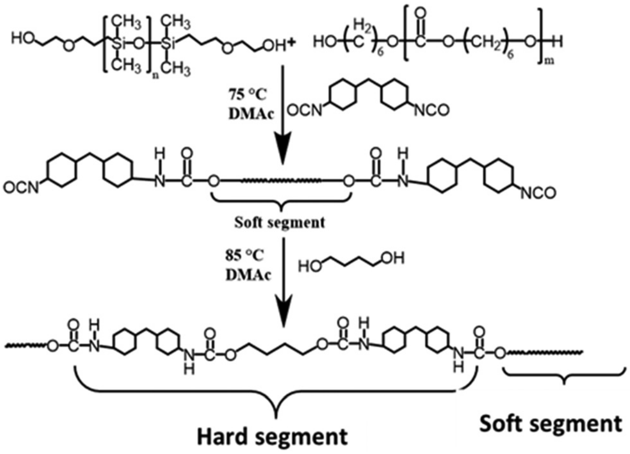

Scheme 1 Preparative pathway of siloxane-based PCUs.

were measured by GPC analysis as depicted in Fig. 1 and the preparative results are summarized in Table 1. Similar to most of the PUs, these siloxane-based PCUs were obtained in yield higher than 85% after thorough purification. All the samples exhibited a nearly unimodal GPC curve with a relatively broader PDI below 2. However, the number average molecular weight (M_n) was gradually decreased from 4.50×10^4 to 3.23×10^4 with increasing molar fraction of PDMS.

As a potential blood-contacting biomaterial, the as-prepared PD20 was selected as a typical siloxane-based PCU to further modify for improving its biocompatibility by incorporating zwitterionic sulfobetaine into its backbones *via* three synthetic protocols: (1) adding MDEA as a co-extender with BDO in a 1 : 1 molar ratio to concomitantly extend the prepolymer chains followed by reacting with PS to form in-chain zwitterions, and (2) and (3) both inserting sulfobetaine diol SB-MDEA as a co-extender with an equal mol% of BDO, but the former utilizing it to initially extend and then BDO to further extend the prepolymer chains, whereas the latter serving the equal mol% of SB-MDEA and BDO to concomitantly extend the prepolymer chains. A schematic description of the synthetic pathways of zwitterionic siloxane-based PCUs is shown in Scheme 2. The molecular weights and PDIs were also determined by GPC analysis as displayed in Fig. 1 and the synthetic results are outlined in Table 1. Similarly, these sulfobetaine modified PCUs presented a nearly unimodal GPC curve with a relatively narrower PDI below 1.61. At the same time, the M_n was reduced from 3.78×10^4 for PD20 to around 2.38×10^4 upon incorporating zwitterionic sulfobetaine. Among the protocols, the first one gave rise to a product with relatively higher M_n and M_w.

Compared to the pristine PCU, the M_n of the resulting siloxane-based PCUs was progressively decreased with increasing molar fraction of PDMS in co-soft segments. This may be due to the poor miscibility of the extremely hydrophobic PDMS component with the relatively hydrophobic PCDL leading to a decrease in the molecular weight. Moreover, after incorporating zwitterionic sulfobetaine into the siloxane-based PCUs *via* three

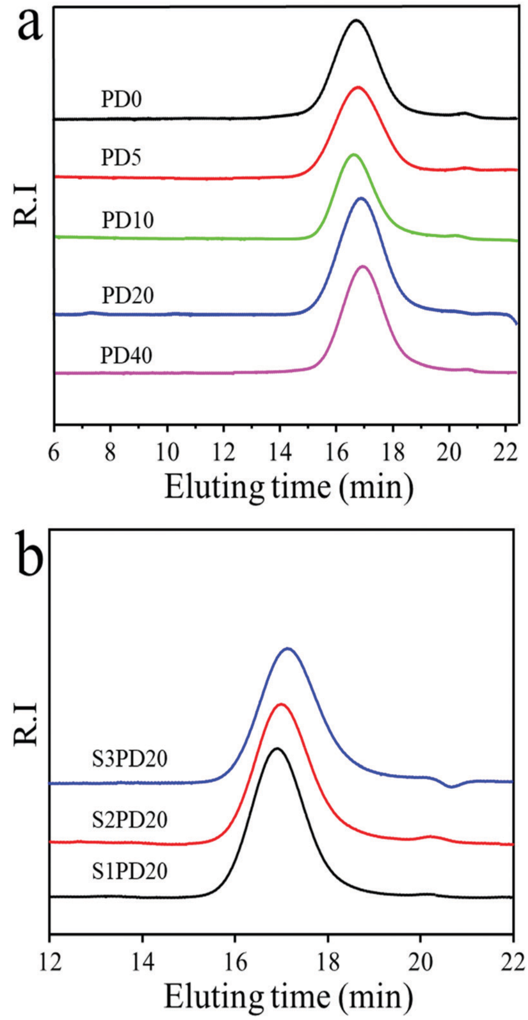

Fig. 1 GPC traces of the siloxane-based PCUs (a) and their sulfobetaine modified ones (b).

protocols, the M_n was further reduced compared to PD20. There were two reasons possibly accounting for this: (1) owing to bulky side chains, MDEA and SB-MDEA as chain extenders do not have a higher reactivity than BDO, so that the chain extension efficiency was lower giving rise to a decrease in the M_n;[37,38] (2) SB-MDEA as a small diol is too polar to be soluble in DMAc, but is soluble in DMSO, so that DMSO instead of DMAc was utilised as a polar solvent to conduct the solution prepolymerisation as evidenced in Fig. S6 (ESI†). However, PDMS is poorly soluble in DMSO and actually both the prepolymerisation of PCDL and PDMS with HMDI and the chain extension using BDO and SB-MDEA were carried out in a heterogeneous state leading to the formation of low Mn sulfobetaine modified siloxane-based PCUs irrespective of adding sequence.[39]

Fig. 2 and Fig. S4 (ESI†) exhibit the FTIR spectra of siloxane-based PCUs, the sulfobetaine modified ones and the raw materials HMDI, PCDL and PDMS. Compared to the spectrum of HMDI, the characteristic absorption peak of isocyanates in all the PUs at 2270 cm^{-1} disappeared completely. Besides the peaks at 2943 and 2848 cm^{-1} ascribed to the stretching

Table 1 Composition, molecular weights and molecular weight distribution of siloxane-based PCUs and their sulfobetaine modified ones

Name	PCDL (mol)	PDMS (mol)	HMDI (mol)	BDO (mol)	MDEA (mol)	PS (mol)	SB-MDEA (mol)	$M_n \times 10^4$	$M_w \times 10^4$	PDI
PD0	1	0	3	2	0	0	0	4.50	8.61	1.91
PD5	0.95	0.05	3	2	0	0	0	3.96	6.40	1.62
PD10	0.9	0.1	3	2	0	0	0	3.91	6.43	1.65
PD20	0.8	0.2	3	2	0	0	0	3.78	7.21	1.91
PD40	0.6	0.4	3	2	0	0	0	3.23	6.21	1.93
S1PD20	0.8	0.2	3	1	1	1	0	2.76	4.29	1.56
S2PD20	0.8	0.2	3	1	0	0	1	2.44	3.76	1.54
S3PD20	0.8	0.2	3	1	0	0	1	1.93	3.12	1.61

vibrations of CH_2 groups in PCDL and the peak at 3319 cm^{-1} assigned to the stretching vibration of N–H in carbamates, the peaks of the carbonyl group (C=O) in carbonates at 1721 cm^{-1} and in carbamates at 1705 cm^{-1}, and the peak of C–N in carbamates at 1541 cm^{-1} also emerged in these samples. Significantly, the characteristic stretching vibration peak of Si–O–Si at 1030 cm^{-1} arising from PDMS got more and more stronger with the increase of PDMS content in the siloxane-based PCUs and this peak was also clearly seen in the sulfobetaine modified ones. These results provided the evidence confirming the successful preparation of siloxane-based PCUs. Although FTIR is a powerful tool to inspect the formation of PUs, it cannot distinguish whether the zwitterionic sulfobetaine was incorporated into the backbones of the siloxane-based PCUs due to the vibration bands at 1058 and 1028 cm^{-1} highly superimposing with the Si–O–Si characteristic stretching vibration bands. The following ^{1}H NMR analysis offered clear evidence supporting the preparation of zwitterionic siloxane-based PCUs.

To distinctly characterize the siloxane-based PCUs and their sulfobetaine modified ones, the structures of PCU0, PD20, S1PD20, S2PD20 and S3PD20 were determined by means of ^{1}H-NMR as shown in Fig. 3 and Fig. S5 (ESI†). As can be seen, the characteristic proton resonance peaks, such as f and k appearing at 3.95–4.00 ppm and ascribed to –O–$C\underline{H}_2$–$(CH_2)_4$–$C\underline{H}_2$–O– in PCDL and b at 3.48–3.52 ppm to –NH–$C\underline{H}(CH)_2$– in HMDI, were clearly visible in the spectrum of PD0. Besides these peaks, new proton resonance peaks, especially q appearing at −0.05 to 0.05 ppm and assigned to –O–$Si(C\underline{H}_3)_2$–, emerged in the spectrum of PD20. Moreover, as for whether zwitterionic sulfobetaine was incorporated into the backbones of the siloxane-based PCUs, typical proton resonance peaks, such as s at 4.39–4.46 ppm to –N^+–CH_2–$C\underline{H}_2$–O– and w at 3.15–3.20 ppm to –N^+–$C\underline{H}_3$, were observed in the spectra of S1PD20, S2PD20 and S3PD20. Taking account altogether of the FTIR and GPC measurements, these results provided the evidence confirming the preparation of siloxane-based PCUs and their sulfobetaine modified ones in this study.

Furthermore, the ^{1}H-NMR analysis also provided information on the zwitterionic ratio or the conversion ratio of MDEA incorporated as a chain extender after reacting with PS. It is highly concerned in the preparation of sulfobetaine modified siloxane-based PCUs *via* the protocol one because the unchanged tertiary amines are prone to the non-specific absorption of proteins as the initiating event in the processes occurring when blood contacts a "foreign" surface in a medical device, inevitably leading to thrombus formation, which is the most serious limitation on the use of blood-contacting biomaterials. The proton resonance peak of pristine –N–$C\underline{H}_3$ appeared at 2.25 ppm as shown in Fig. S2 (ESI†), and the protonated –N^+–$C\underline{H}_3$ shifted to 3.15–3.20 ppm as exhibited in Fig. 3. Based on the integrated area of the corresponding protons, the zwitterionic ratio of the protocol one was calculated to be ∼75%. This result is in accordance with the literature.[34]

Mechanical property measurements

The stress–strain curves of the siloxane-based PCUs and the corresponding zwitterionic ones are illustrated in Fig. 4, and the measurement results are summarized in Table 2. At the same time, the fracture energy (G_F) was estimated from the area under stress–strain curves. Like most of the PUs, the mechanical properties of these siloxane-based PCUs and the zwitterionic ones were closely related to their molecular weight. As the M_n displayed a decreasing trend with the molar fraction of PDMS, the ultimate tensile strength (σ_m) of siloxane-based PCUs behaved similarly. For example, the σ_m was decreased from 54.88 MPa in PD0 to 38.39 MPa in PD40, whereas this value was suddenly dropped from 43.11 MPa in PD20 to about 25.26 MPa in the resulting PCUs.

Other mechanical properties, such as Young's modulus (E), elongation at break (ε_b) and fracture energy (G_F), also depicted a gradually decreasing trend with the increase of PDMS content.

As mentioned above, a gradually decreased molecular weight contributed to a progressively decreased σ_m in the siloxane-based PCUs and an introduction of zwitterionic sulfobetaine led to a sudden drop of σ_m in the zwitterionic modified ones. For the siloxane-based PCUs, this was mainly caused by the following reasons: (1) the miscibility between non-polar PDMS and extremely polar urethane components was poor, which deepened the microphase separation resulting in the decrease of mechanical properties; (2) the mechanical properties of PDMS itself were inferior to that of PCDL. Upon replacing part of PCDL using PDMS, the overall mechanical properties would be deteriorated; (3) from the GPC analysis, the molecular weight decreased with the increase of PDMS content, which would lead to less entanglement between macromolecule chains impairing the mechanical properties. For the zwitterion modified PCUs, there were two reasons accounting for this: (1) due to the presence of sulfobetaine,

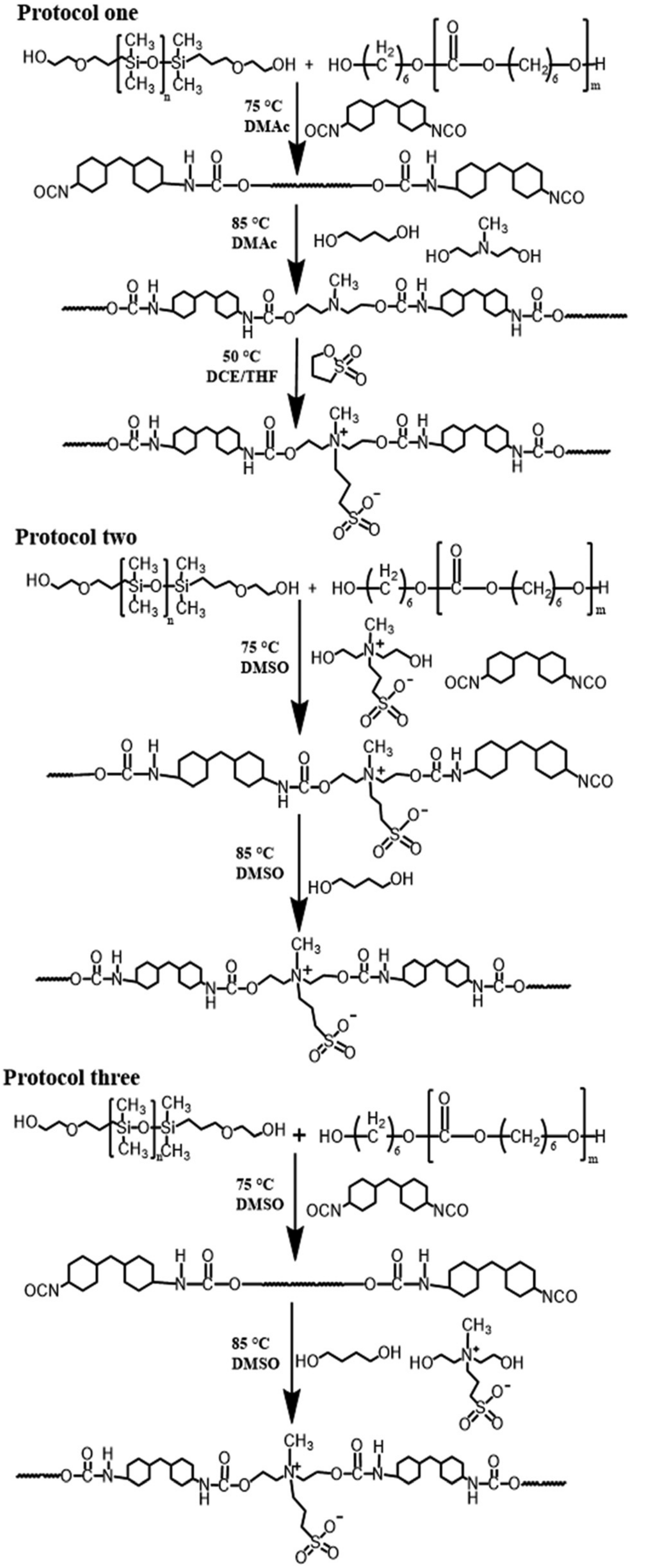

Scheme 2 Synthetic pathways of sulfobetaine modified siloxane-based PCUs *via* three protocols.

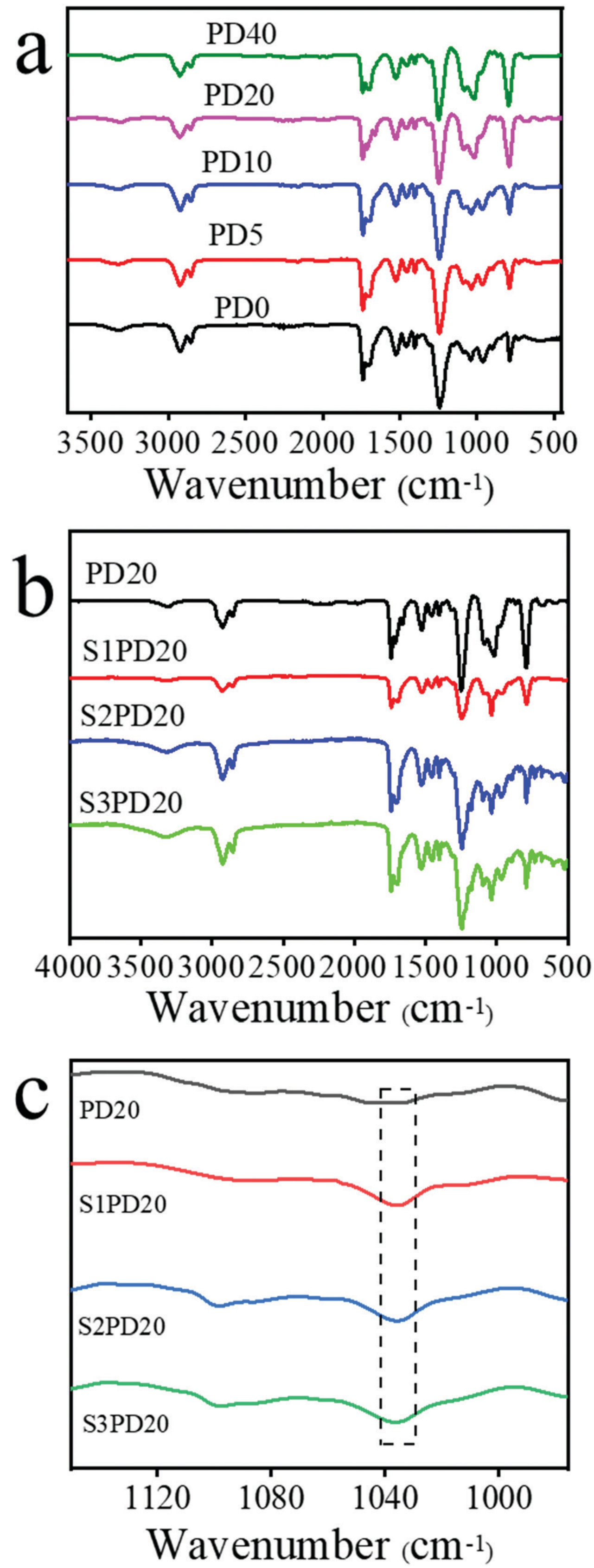

Fig. 2 FTIR spectra of the siloxane-based PCUs (a) and their sulfobetaine modified ones (b and c).

the accumulation of the hard segment is destroyed, resulting in the reduction of hydrogen bonds between the hard segments to depress the degree of microphase separation and the

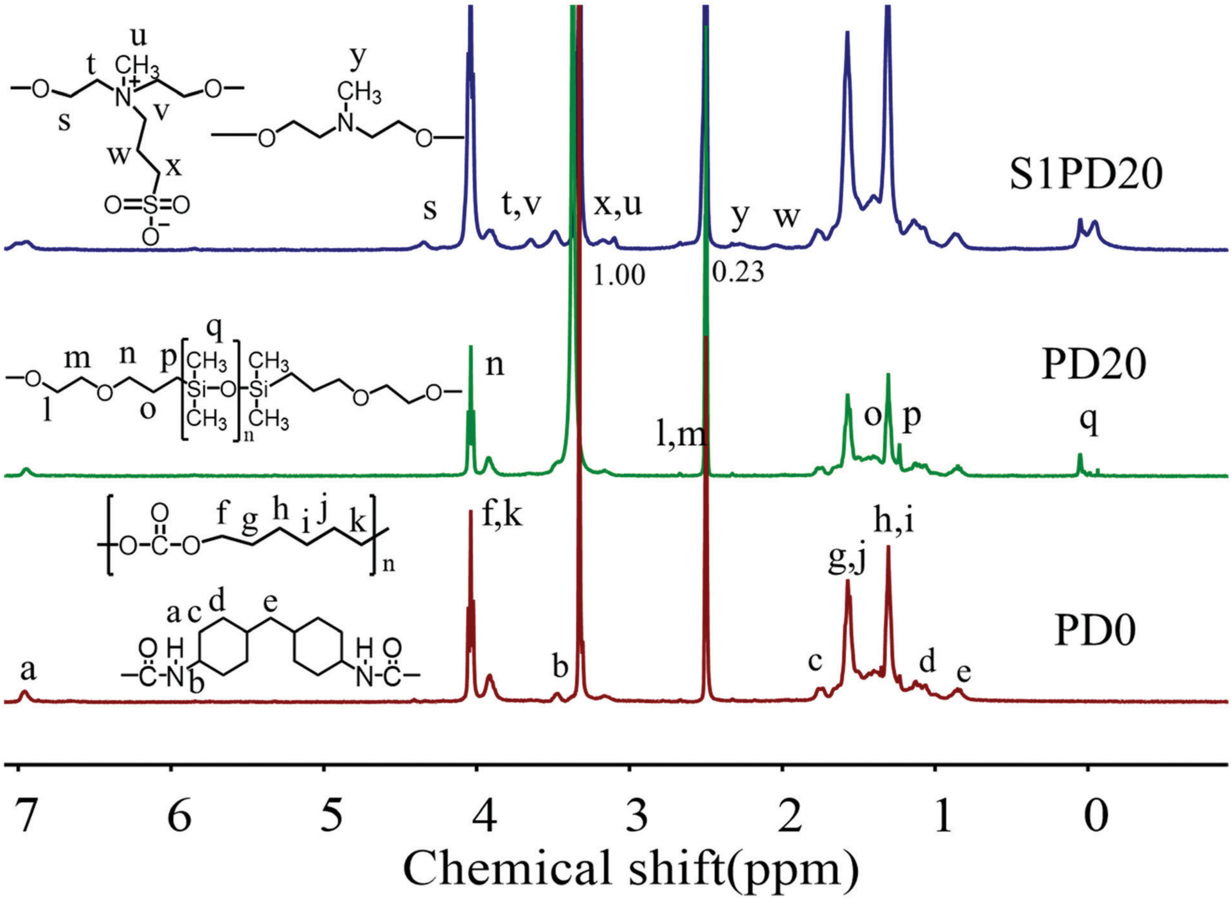

Fig. 3 ^{1}H-NMR spectra of PCU0, PD20 and S1PD20 in DMSO-d$_6$.

mechanical properties;[40] (2) a significant decrease in M_n gave rise to a marked decrease in the degree of entanglement between the macromolecular chains to lower the mechanical properties of the zwitterionic PCUs.[41]

To gain further insight into the effect of incorporating zwitterions on the microphase structure of siloxane-based PCUs, DMA analysis was carried out and the testing results are shown in Fig. 5 and the testing results are summarized in Table 3. These measurements provided information on the glass transition, phase separation, and mechanical behaviour of the sulfo-betaine modified PCUs as a function of temperature under dynamic conditions. As can be seen, the storage modulus (E') of the unmodified PD20 was lower than those of both S1PD20 and S2PD20 in the range of −120 °C to 30 °C, but was higher than that of S3PD20. However, in the glass transition region of PCDL in the range of −30 °C to 30 °C, the E' of S3PD20 became higher than that of PD20, while those of both S1PD20 and S2PD20 still remained higher than that of PD20. Upon going into the rubber state, the E' of S1PD20 and S3PD20 rapidly dropped to a very low level, but S2PD20 still remained significantly higher, reaching 492.8 MPa at 30 °C, 6.67 times higher than 73.9 MPa in PD20. This increase in the E' of the resulting zwitterionic PCUs suggested that the ionic clusters formed from supra-molecular assembly of zwitterions acted as a reinforcing agent more efficiently through enhanced macro-phase separation after the incorporation of sulfobetaine, even though these PCUs possessed a suddenly decreased molecular weight. The formation of ionic clusters between the incorporated sulfobetaine zwitterions was also supported by the appearance of molecular ionic peaks of the dimers and trimers in the mass spectrum of SB-MDEA as displayed in Fig. S3 (ESI†). Furthermore, S2PD20 maintained a persistently higher E' than others from the glass state to the viscous flow state and both S1PD20 and S3PD20 showcased a suddenly dropped E' in the rubber state. This was in good agreement with the highest Young's modulus recorded in S2PD20 among all the PCUs in this study.

As shown in Fig. 5(b), two peaks appeared in the tan δ *vs.* temperature curve of PD20 corresponding to two phase morphologies arising from a well-defined PDMS T_g at about −113 °C and PCDL T_g at around −10 °C, respectively. As seen in Table 3, the T_g coming from PDMS remained nearly unchangeable in S1PD20 and S3PD20, whereas this value was slightly increased to −110 °C in S2PD20. Meanwhile, the T_g coming from PCDL was increased to −5.9 to −7.1 °C in S1PD20 and S2PD20, whereas it was decreased to −12.3 °C in S3PD20. These results indicated that the ionic clusters created from supramolecular assembly of zwitterions are seldom incompatible with the PDMS and PCDL co-soft segments.

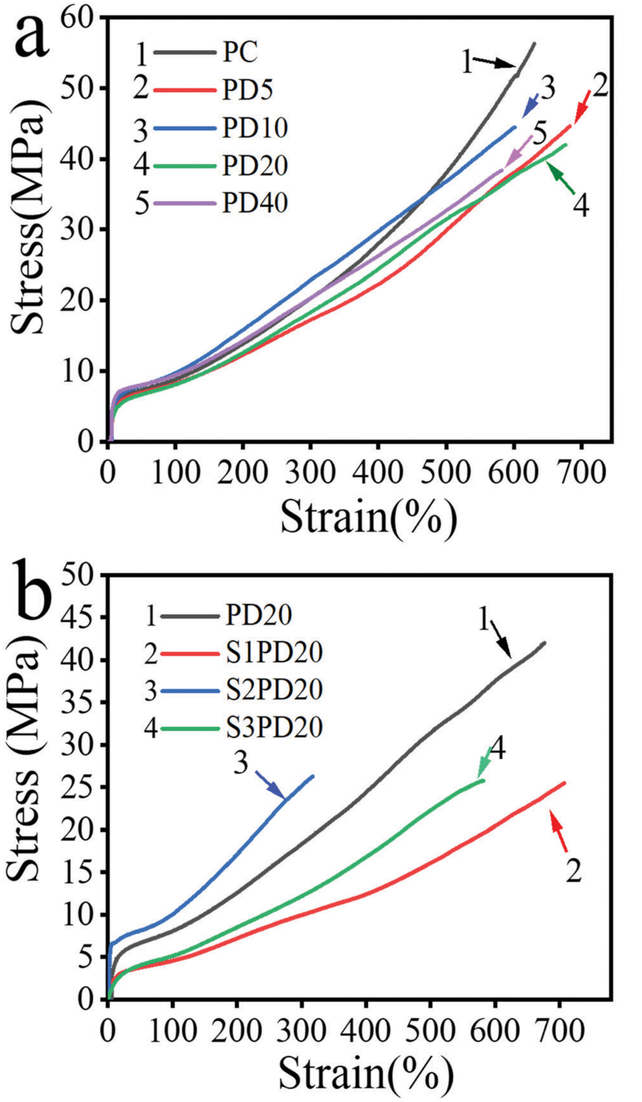

Fig. 4 Stress–strain curves of siloxane-based PC PUs (a) and their sulfobetaine modified ones (b).

Table 2 The strain–stress results of siloxane-based PC PUs and their sulfobetaine modified ones

Name	E (MPa)	σ_m (MPa)	ε_b (%)	G_F (MN m^{-1})
PD0	30.2 ± 2.1	54.9 ± 2.5	621 ± 21	152.3 ± 22.4
PD5	25.6 ± 1.5	46.1 ± 2.3	699 ± 14	145.7 ± 19.1
PD10	34.0 ± 1.1	43.2 ± 3.4	621 ± 18	139.9 ± 22.5
PD20	24.8 ± 2.1	43.1 ± 3.0	623 ± 47	146.4 ± 36.7
PD40	41.3 ± 3.2	38.4 ± 3.1	578 ± 52	119 ± 30.2
S1PD20	13.3 ± 0.8	25.4 ± 0.9	662 ± 48	86.4 ± 17.8
S2PD20	87.6 ± 1.3	25.9 ± 0.4	327 ± 46	47.7 ± 14.3
S3PD20	14.5 ± 1.8	24.5 ± 1.2	574 ± 7	75.4 ± 7.9

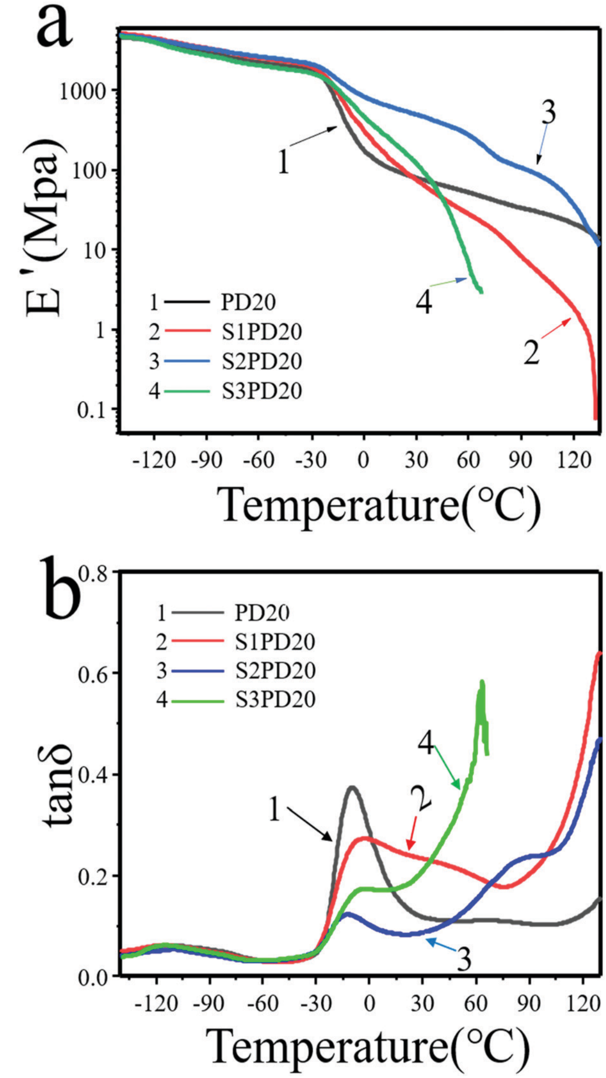

Fig. 5 Dynamic-mechanical spectra of the siloxane-based PCUs and their sulfobetaine modified ones. (a) E' and (b) $\tan\delta$ *vs.* T.

Table 3 E' and T_g of the siloxane-based PCUs and their sulfobetaine modified ones

Sample	PD20	S1PD20	S2PD20	S3PD20
T_g (°C)	−115.8	−116.1	−109.7	−114.2
$\tan\delta$	0.06	0.06	0.04	0.06
T_g (°C)	−10	−7.1	−5.9	−12.3
$\tan\delta$	0.37	0.27	0.17	0.12
E' (MPa, 0 °C)	177.3	311.1	833.4	469.6
E' (MPa, 20 °C)	93.7	111.5	574.4	195.5
E' (MPa, 37 °C)	71.1	57.3	441.3	78.9
E' (MPa, 60 °C)	52.1	27.7	271.9	6.5

Surface/interface composition and hydrophobicity

The surface and interface chemical analysis would provide information about the enhancement of the biostability of PCUs after the incorporation of silicone and further zwitterionic modification. The surface chemical compositions of siloxane-based PCUs and their sulfobetaine modified ones were analysed by XPS. The results tested at a take-off angle of 90° corresponding to element detection at a depth of 10 nm are summarized in Table 4. The surface atom contents of nitrogen (N) and silicon (Si) represented the fractions of hard segments and PDMS, respectively. Upon incorporating PDMS, the Si element was detected immediately,

Table 4 XPS analytical results of the siloxane-based PCUs and their sulfobetaine modified ones

Sample	Depth (nm)	C (%)	N (%)	O (%)	Si (%)	Si (theo. %)	S (theo. %)	S (%)
PD0	10	71.30	3.24	25.47	0	0	0	—
PD5	10	60.10	2.05	27.44	10.41	0.66	0	—
PD10	10	60.35	1.78	24.72	13.15	1.32	0	—
PD20	10	57.23	0.75	27.18	14.84	2.68	0	—
PD40	10	50.82	1.99	27.87	19.31	5.28	0	—
S1PD20	10	60.67	1.97	24.83	11.76	2.66	0.69	0.60
S2PD20	10	66.66	1.30	23.69	7.77	2.66	0.69	0.43
S3PD20	10	64.07	2.11	23.89	8.48	2.66	0.69	0.46

and the Si content found on the surface of silicone-based PCUs was substantially higher than that in the bulk. For example, the percentage of the surface Si element was increased from 0% to 19.31% as the molar fraction of PDMS doped in the co-soft segments was increased from 0% to 40%. This revealed that a vast amount of PDMS can migrate through the bulk to the surface making a great contribution to the biostability due to low surface energy.

To further verify the unique migration of PDMS, the surface and interface chemical analysis of PD20 was carried out *via* variable angle tests and the results are displayed in Fig. 6a. The take-off angles used were $\sin\alpha = 1$, $\sin\alpha = 0.7$ and $\sin\alpha = 0.4$ corresponding to element detection at depths of 10 nm, 7 nm and 4 nm, respectively. As the detection depth was decreased, the Si element tested showed an obvious increasing trend as schematically described by the molecular model presented in Fig. 6b. This was because the Si element migrated to the surface which would protect the material body like a shell from the attack of water molecules and active oxygen species. Moreover, in the sulfobetaine modified siloxane-based PCUs *via* the three synthetic protocols, apart from that the surface Si element was clearly detected, the found content of the surface Si element was also substantially higher than the theoretical value. For example, the content of the surface Si element was decreased from 14.84% in PD20 to 11.76% in S1PD20, 7.77% in S2PD20 and 8.48% in S3PD20. This may be explained by the following reasons: (1) the introduction of the S element reduced the proportion of other elements; (2) the tethering of sulfobetaine depressed both the degree of microphase separation[40] and the degree of Si element migration to the surface. Nevertheless, the sulfobetaine modified siloxane-based PCUs created *via* protocols two and three should have a perfect zwitterionic ratio due to SB-MDEA directly integrating into their backbones. In fact, a relatively lower S element content was found in S2PD20 and S3PD20 compared to S1PD20. It was most likely due to a poor miscibility of SB-MDEA with PDMS in DMSO leading to a relatively lower incorporation of both SB-MDEA and PDMS as demonstrated in Fig. S6 (ESI†).

The WCA test was further exploited to inspect the effects of incorporating PDMS and zwitterions on the surface hydrophobic/hydrophilic properties of PCUs as potential blood-contacting bio-materials. As shown in Fig. 7a and Tables S1 and S2 (ESI†), the WCA was gradually increased from 94.3° in PD0 to 116.8° in PD40 as the molar fraction of PDMS was

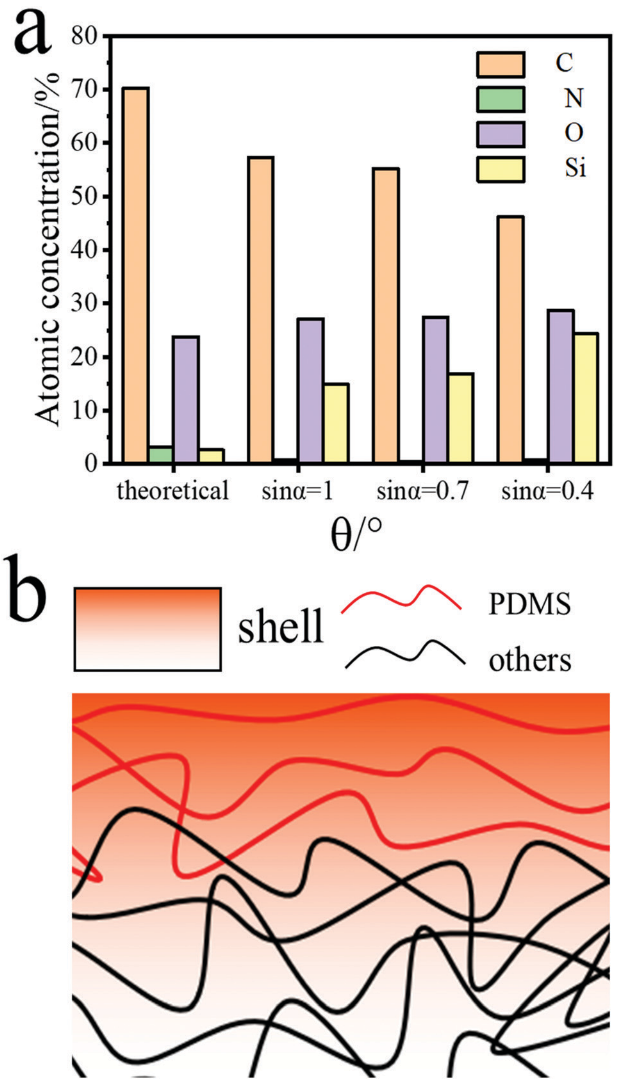

Fig. 6 XPS analysis of PD20 from different angles (a) and molecular model (b).

increased from 0% to 40%. This clearly resulted from the enrichment of Si elements on the surface of siloxane-based PCUs markedly contributing to a higher hydrophobicity due to the low surface energy of PDMS. After sulfobetaine was incorporated into PD20, the WCA was again dropped to approximately 94°, suggesting that the hydrophilicity improved. Furthermore, when S1PD20–S3PD20 were placed in the air atmosphere for 0, 3, 6 and 10 days respectively, their WCA remained nearly unchanged over time, showing the stable phase-separation structure and surface/interface composition. In view of the unusually high surface Si content and hydrophilicity enhancement obtained by uniquely inserting silicone and sulfobetaine, these PCUs displayed great potential to be used as blood-contacting biomaterials with excellent biostability and biocompatibility.

In addition, the water uptake of the siloxane-based PCUs and their sulfobetaine modified ones was also determined and the results are exhibited in Fig. 7b. PD0 possessed a relatively

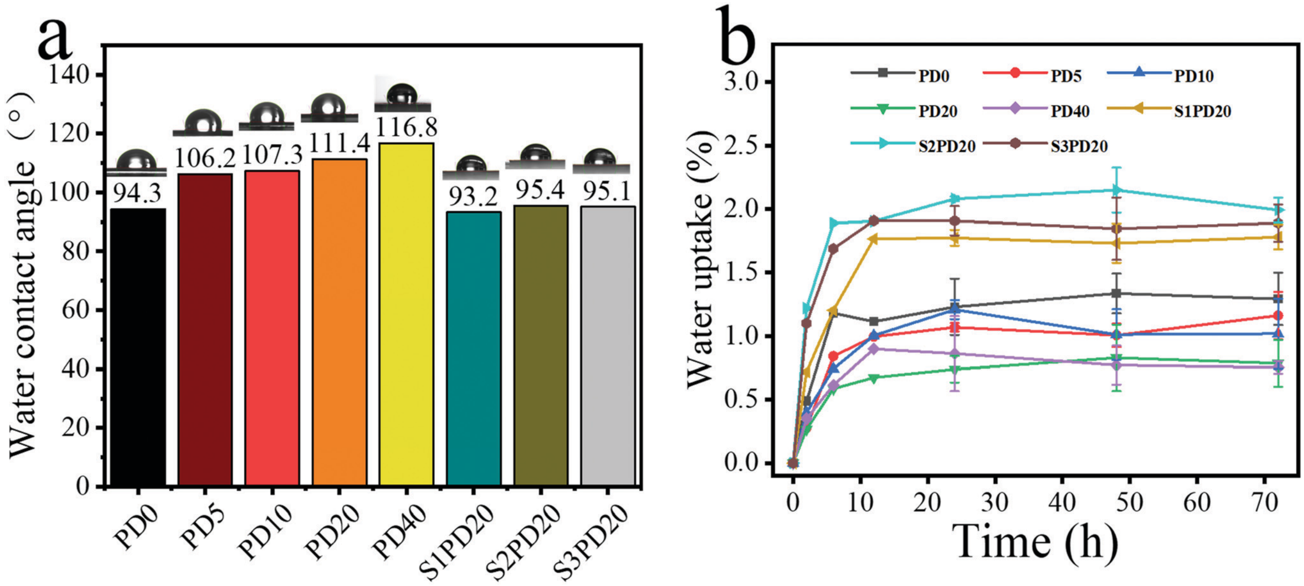

Fig. 7 Water contact angle of series polyurethane (a); water absorption curve of series polyurethane (b).

higher equilibrium water uptake below 1.5%, and this value was further decreased with the molar fraction of PDMS in the co-soft segments varying from 5% to 40%. However, after the zwitterion modification, the equilibrium water uptake was slightly increased to the range of 1.5%–2.0%. These results also provided the evidence supporting that incorporating PDMS indeed improves the hydrophobicity of the PCUs, whereas introducing sulfobetaine zwitterions again impart them the hydrophilicity.

Evaluation of blood compatibility

The hemolysis test is frequently performed to assess the integrity of red blood cells (RBC) in direct contact with the synthetic polymer materials. During a hemolytic process, rupture of red blood cells will leak free hemoglobin, and intracellular components and thrombotic substances will enter the plasma, which in turn activates the coagulation cascade, leading to thrombosis. In the hemolysis test, the amount of free hemoglobin in plasma was analysed using a spectrophotometer. According to ISO/TR 7406, the critical safety limit for hemolysis of biomaterials is less than 5%. The blood hemolytic photographs of the selected PD20 and its sulfobetaine modified counterparts in direct contact with blood are shown in Fig. 8a, and the inset shows a photograph of blood after centrifugation. The positive control Triton showed 100% hemolysis, while the negative control saline displayed no hemolysis. The hemolysis ratio of all the experimental samples was less than 1.5%. Evidently, the siloxane-based PCUs and their sulfobetaine modified ones presented excellent blood compatibility.

To evaluate the influence of the selected PD20 and its sulfobetaine modified counterparts on the external and internal pathways of coagulation activation, their APTT was determined and the results are illustrated in Fig. 8b. According to the literature,[23,24] APTT measurement is usually carried out as follows. Under the condition of 37 °C, kaolin activating factors XII and cephalin (partial thromboplastin) were used instead of the platelet third factor, observing plasma coagulation with the participation of Ca^{2+}. The required time, the so-called APTT, is the most sensitive and most commonly used screening test in the endogenous coagulation system. As an effective way to detect endogenous coagulation, APTT is more sensitive to the lack or increase of endogenous coagulation pathway factors (VIII, I, and XI),[42,43] but is not sensitive enough to the detection of prothrombin and fibrinogen. In fact, the APTT values of the control group and the experimental groups were both around 75 seconds. Therefore, the addition of zwitterionic sulfobetaine as an effective method to reduce the adsorption of non-specific proteins and platelet adhesion to reduce thrombosis[33,44,45] may have a relatively limited contribution to APTT.

The adsorption of proteins on biomaterials is the first step for the following coagulation cascade reactions, so the anti-adsorption of proteins is very important in the design and preparation of anti-coagulation blood-contacting biomaterials. Fig. 8c exhibits the non-specific adsorption testing results of fibrinogen on PD20 and its sulfobetaine modified counterparts. After incorporating zwitterions into the siloxane-based PCUs, the amount of protein adsorption was in the range of 3.5–4.0 $\mu g\ cm^{-2}$, substantially lower than the sulfobetaine unmodified sample. There was no statistical difference between these sulfobetaine modified siloxane-based PCUs. This may be due to the fact that the zwitterions form a ''hydration layer'' on the surface of siloxane-based PCUs to hinder the adsorption of protein. As is well recognised, when a biomaterial is immersed in the blood, fibrinogen is adsorbed on the surface, promoting platelet adhesion, and then the platelets are agglomerated and activated, leading to thrombus formation. Consequently, the reduction of non-specific protein adsorption would make a major contribution to the reduction of platelet adhesion. For

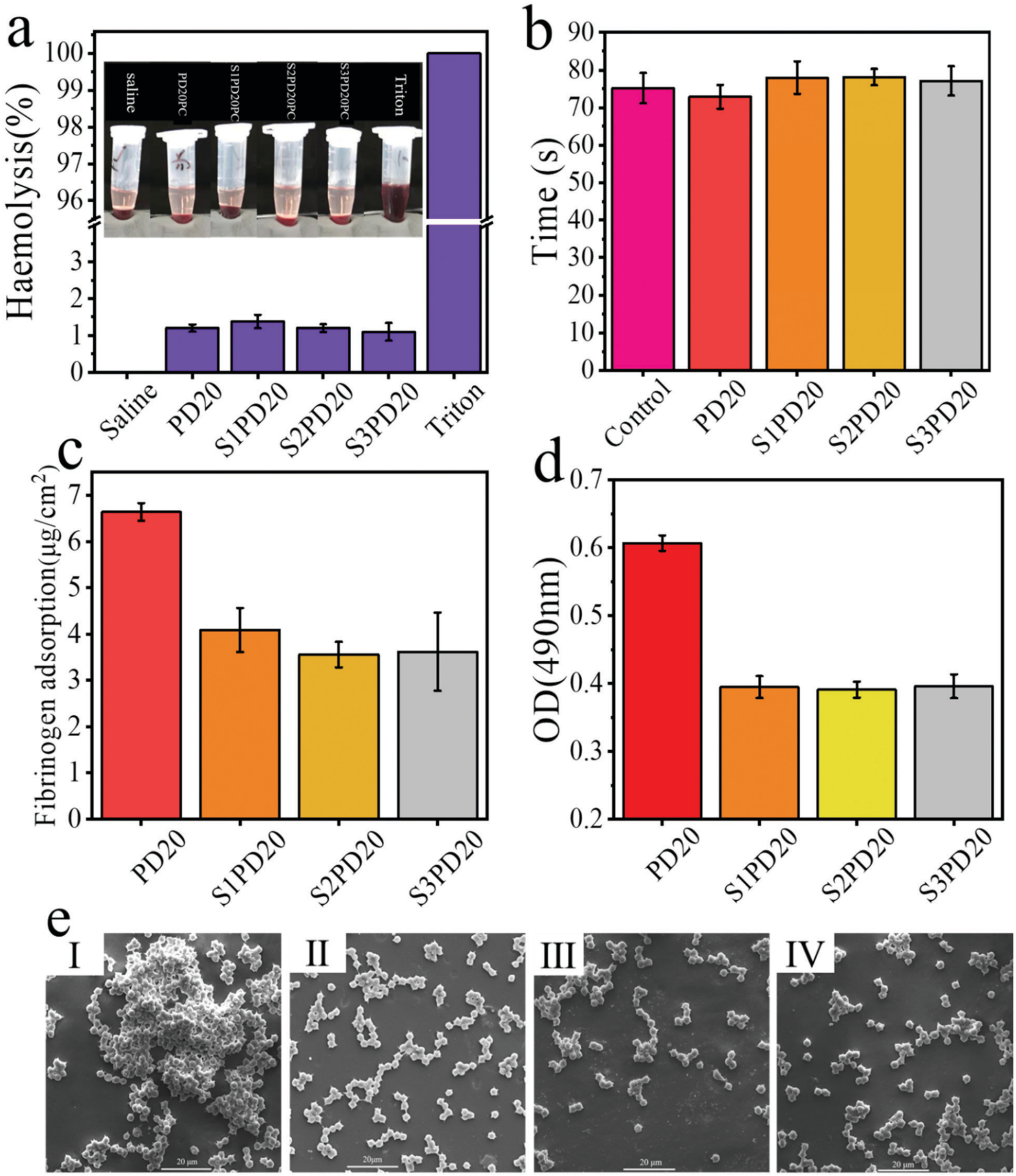

Fig. 8 Hemolysis experiment (a), change of APTT (b), non-specific protein adsorption test results (c), the number of platelets adsorbed on PD20 and its sulfobetaine modified counterparts (d) and SEM images of platelets adhered on PD20 (I), S1PD20 (II), S2PD20 (III) and S3PD20 (IV) (e).

a semi-quantitative analysis, the LDH method was used to determine the number of platelets adsorbed on the surface of PD20 and S1PD20–S3PD20 as shown in Fig. 8d. Upon inserting zwitterions into the siloxane-based PCUs, the OD value got lower than the original PD20, which that meant these sulfobetaine modified PCUs possess lower platelet adhesion. However, they show-cased nearly no statistical difference in the OD values. The number and morphology of platelets adsorbed were also evidenced by SEM observation as depicted in Fig. 8e. As seen, there was an obvious difference between PD20 and its sulfobetaine modified counterparts. PD20 had demonstrated clear platelet aggregation, but these sulfobetaine modified PCUs revealed only a little platelet aggregation. This was in good agreement with their OD testing results. As a result, introducing zwitterions inhibited the adhesion of fibrinogen, thereby achieving the purpose of limiting platelet adhesion and formation of thrombosis.

Conclusions

In this study, silicone-modified PCUs were synthesized and characterized. When a molar fraction of PDMS in the co-soft segments was greater than 20%, the as-prepared PCUs displayed better biostability, but the mechanical properties got decreased. In order to further improve the biocompatibility, the zwitterionic sulfobetaine was incorporated into their backbones. Although the molecular weight was further depressed after the zwitterionic modification, the fibrinogen absorption on and platelet adhesion to the surface of these zwitterionic PCUs were significantly inhibited showing great potential to meet the requirements of practical applications as blood-contacting biomaterials.

Author contributions

Zhi-hua Liu: methodology, investigation, data analysis, writing-original draft. Yong-hao Xiao: methodology, investigation. Xiao-yu Ma: methodology, investigation. Xue Geng: investigation, validation. Lin Ye: investigation, validation. Ai-ying Zhang: supervision, validation. Zeng-guo Feng: conceptualization, supervision, funding acquisition, methodology, writing-review and editing.

Conflicts of interest

There are no conflicts to declare.

Acknowledgements

This work was financially supported by the National Key R&D Program of China (2017YFC1104101).

References

1 P. A. Gunatillake, L. S. Dandeniyage, R. Adhikari, M. Bown, R. Shanks and B. Adhikari, *Polym. Rev.*, 2018, **59**, 391–417.
2 D.-W. Ma, R. Zhu, Y.-Y. Wang, Z.-R. Zhang and X.-Y. Wang, *Front. Mater. Sci.*, 2015, **9**, 397–404.
3 A. A. Gostev, A. A. Karpenko and P. P. Laktionov, *Polym. Bull.*, 2018, **75**, 4311–4325.
4 E. M. Christenson, M. Dadsetan, M. Wiggins, J. M. Anderson and A. Hiltner, *J. Biomed. Mater. Res. A*, 2004, **69**, 407–416.
5 G. Soldani, P. Losi, M. Bernabei, S. Burchielli, D. Chiappino, S. Kull, E. Briganti and D. Spiller, *Biomaterials*, 2010, **31**, 2592–2605.
6 E. M. Christenson, J. M. Anderson and A. Hiltner, *Corros. Eng., Sci. Technol.*, 2013, **42**, 312–323.
7 K. A. Chaffin, X. Chen, L. McNamara, F. S. Bates and M. A. Hillmyer, *Macromolecules*, 2014, **47**, 5220–5226.
8 P. A. Gunatillake, D. J. Martin, G. F. Meijs, S. J. McCarthy and R. J. Adhikari, *Aust. J. Chem.*, 2003, **56**, 545–557.
9 A. Simmons, J. Hyvarinen, R. A. Odell, D. J. Martin, P. A. Gunatillake, K. R. Noble and L. A. Poole-Warren, *Biomaterials*, 2004, **25**, 4887–4900.
10 E. M. Christenson, M. Dadsetan and A. Hiltner, *J. Biomed. Mater. Res. A*, 2005, **74**, 141–155.
11 A. Simmons, J. Hyvarinen and L. Poole-Warren, *Biomaterials*, 2006, **27**, 4484–4497.
12 E. M. Christenson, M. Dadsetan, J. M. Anderson and A. J. Hiltner, *Jpn. Soc. Biomater.*, 2005, **74**, 141–155.
13 X. Xie, A. Eberhart, R. Guidoin, Y. Marois, Y. Douville and Z. Zhang, *J. Biomater. Sci., Polym. Ed.*, 2010, **21**, 1239–1264.
14 J. Yang, Y. Gao, J. Li, M. Ding, F. Chen, H. Tan and Q. Fu, *RSC Adv.*, 2013, **3**, 8291–8297.
15 R. Zhu, X. Wang, J. Yang, Y. Wang, Z. Zhang, Y. Hou and F. Lin, *Biomed. Mater.*, 2016, **12**, 015011.
16 R. Zhu, Y. Wang, Z. Zhang, D. Ma and X. Wang, *Heliyon*, 2016, **2**, e00125.
17 Y. Li, L. Yuan, H. Ming, X. Li, L. Tang, J. Zhang, R. Wang, G. Wang, Y. Jiang, Z. Li, F. Luo, J. Li, H. Tan and Q. Fu, *Biomacromolecules*, 2020, **21**, 1460–1470.
18 J. A. Jones, M. Dadsetan, T. O. Collier, M. Ebert, K. S. Stokes, R. S. Ward, P. A. Hiltner and J. M. Anderson, *J. Biomater. Sci., Polym. Ed.*, 2004, **15**, 567–584.
19 T. Sun, H. Tan, D. Han, Q. Fu and L. Jiang, *Small*, 2005, **1**, 959–963.
20 X. Hou, X. Wang, Q. Zhu, J. Bao, C. Mao, L. Jiang and J. Shen, *Colloids Surf., B*, 2010, **80**, 247–250.
21 S. Nie, J. Xue, Y. Lu, Y. Liu, D. Wang, S. Sun, F. Ran and C. Zhao, *Colloids Surf., B*, 2012, **100**, 116–125.
22 R. Biran and D. Pond, *Adv. Drug Delivery Rev.*, 2017, **112**, 12–23.
23 X. Jin, X. Geng, L. Jia, Z. Xu, L. Ye, Y. Gu, A. Y. Zhang and Z. G. Feng, *Macromol. Biosci.*, 2019, **19**, e1900114.
24 X. Hui, X. Geng, L. Jia, Z. Xu, L. Ye, Y. Gu, A. Y. Zhang and Z. G. Feng, *J. Biomater. Appl.*, 2020, **34**, 812–826.
25 C.-C. Lien, P.-J. Chen, A. Venault, S.-H. Tang, Y. Fu, G. V. Dizon, P. Aimar and Y. Chang, *J. Membr. Sci.*, 2019, **584**, 148–160.
26 F. Yang, L. Xu, D. Kuang, Y. Ge, G. Guo and Y. Wang, *Chem. Eng. J.*, 2021, **410**, 128244.
27 Y. M. Thasneem, M. R. Rekha, S. Sajeesh and C. P. Sharma, *J. Colloid Interface Sci.*, 2013, **409**, 237–244.
28 Y. Zhang, X. S. Li, A. G. Guex, S. S. Liu, E. Muller, R. I. Malini, H. J. Zhao, M. Rottmar, K. Maniura-Weber, R. M. Rossi and F. Spano, *Biofabrication*, 2017, **9**, 025010.
29 P. W. Raut, A. A. Shitole, A. Khandwekar and N. Sharma, *J. Mater. Sci.*, 2019, **54**, 10457–10472.
30 S. Kudaibergenov, W. Jaeger and A. Laschewsky, *Supramolecular Polymers Polymeric Betains Oligomers*, 2006, ch. 78, pp. 157–224, DOI: 10.1007/12_078.
31 R. S. Smith, Z. Zhang, M. Bouchard, J. Li, H. S. Lapp, G. R. Brotske, D. L. Lucchino, D. Weaver, L. A. Roth, A. Coury, J. Biggerstaff, S. Sukavaneshvar, R. Langer and C. Loose, *Sci. Transl. Med.*, 2012, **4**, 153ra132.

32 H. J. Kwon, Y. Lee, L. T. Phuong, G. M. Seon, E. Kim, J. C. Park, H. Yoon and K. D. Park, *Acta Biomater.*, 2017, **61**, 169–179.

33 S. Kim, S. H. Ye, A. Adamo, R. A. Orizondo, J. Jo, S. K. Cho and W. R. Wagner, *J. Mater. Chem. B*, 2020, **8**, 8305–8314.

34 S. H. Ye, C. A. Johnson, Jr., J. R. Woolley, H. Murata, L. J. Gamble, K. Ishihara and W. R. Wagner, *Colloids Surf., B*, 2010, **79**, 357–364.

35 W. H. Kuo, M. J. Wang, H. W. Chien, T. C. Wei, C. Lee and W. B. Tsai, *Biomacromolecules*, 2011, **12**, 4348–4356.

36 S. H. Ye, Y. Hong, H. Sakaguchi, V. Shankarraman, S. K. Luketich, A. D'Amore and W. R. Wagner, *ACS Appl. Mater. Interfaces*, 2014, **6**, 22796–22806.

37 L. Yang, Y. Wang and X. Peng, *J. Macromol. Sci., Part A*, 2017, **54**, 516–523.

38 J. W. Li, H. T. Lee, H. A. Tsai, M. C. Suen and C. W. Chiu, *Polymers*, 2018, **10**, 1292.

39 A. Penhasi, M. Aronhime and D. Cohn, *Polymers of Biological and Biomedical Significance*, 1993, pp. 87–102, DOI: 10.1021/bk-1994-0540.ch008.

40 X. Li, F. Ye, J. Ouyang, Z. Chen and X. Yang, *Polymer*, 2021, **237**, 124303.

41 Z. Li, J. Yang, H. Ye, M. Ding, F. Luo, J. Li, J. Li, H. Tan and Q. Fu, *Biomacromolecules*, 2018, **19**, 2137–2145.

42 J. Cao, M. Yang, A. Lu, S. Zhai, Y. Chen and X. Luo, *J. Biomed. Mater. Res. A*, 2013, **101**, 909–918.

43 T. Liu, Y. Liu, Y. Chen, S. Liu, M. F. Maitz, X. Wang, K. Zhang, J. Wang, Y. Wang, J. Chen and N. Huang, *Acta Biomater.*, 2014, **10**, 1940–1954.

44 D. H. Ga, C. M. Lim, Y. Jang, T. I. Son, D. K. Han and Y. K. Joung, *Tissue Eng. Regen. Med.*, 2022, **19**, 35–47.

45 Q. Liu, X. Wang, A. Chiu, W. Liu, S. Fuchs, B. Wang, L. H. Wang, J. Flanders, Y. Zhang, K. Wang, J. M. Melero-Martin and M. Ma, *Adv. Mater.*, 2021, **33**, e2102852.